

Effect of Inter-Cavity Spacing and Heat Treatment in Friction Stir Processing/Welding (FSP/FSW) Al7075 Composites Containing Al₂O₃ and Graphene Nanomaterials using Charpy Impact Test

Ali Hossein zadeh^{1, *}, Mahmood Shariati²

Department of Mechanical Engineering,
Ferdowsi University of Mashhad, Iran

E-mail: a.hosseinzadeh.PhD@mail.um.ac.ir, mshariati44@um.ac.ir

*Corresponding author

Danial Ghahremani-moghadam³

Department of Mechanical Engineering,
Quchan University of Technology

E-mail: d.ghahremani@qiet.ac.ir

Mohammad Reza Maraki⁴

Department of Material Engineering,
Birjand University of Technology

E-mail: maraki@birjandut.ac.ir

Received: 23 October 2021, Revised: 28 March 2022, Accepted: 31 March 2022

Abstract: In this research, the friction stir process by adding Al₂O₃ and graphene nanoparticles at two different distances have been investigated. Nanoparticles are inserted in cavities with a diameter of 2 mm and a depth of 3 mm. Nanoparticles of Al₂O₃, graphene, and equal compositions of Al₂O₃ and graphene, each with two cavity spacings of 8 and 10 mm, have been performed in six different groups of friction stir process. From each group, Six Charpy specimens were separated. Charpy impact test was performed on six samples, three of which were heat-treated after the friction stir process. Charpy impact test has shown that the specimens have higher fracture energy after heat treatment. Also, in all cases, the fracture energy at the distance between the two cavities are 10 mm more than the distance of 8 mm, this is since nanoparticles do not accumulate at a more distance. Also, to observe the resulting microstructures using optical microscopy and scanning electron microscopy on the friction welding process and the fracture surface of Charpy impact specimens were performed. The results show that the nanoparticles are accumulated in some samples and well dispersed in the materials in others.

Keywords: Aluminum Matrix Composites, Al₂O₃, Charpy Impact Test, Friction Stir Processing, Grapheme, Nanoparticle

Biographical notes: Ali Hosseinzadeh is a PhD candidate at Ferdowsi University of Mashhad, Iran. His main research interests are fatigue, fracture and impact mechanic. Mahmood Shariati received his PhD in Mechanical Engineering from Tarbiat Modares University, Iran in 1999. He is currently Full Professor at the Department of Mechanical Engineering in Ferdowsi University of Mashhad, Iran. Danial Ghahremani-moghadam received his PhD in Mechanical Engineering from Ferdowsi University of Mashhad, Iran in 2016. He is currently Assistant Professor at the Department of Mechanical Engineering in Quchan University of Technology, Iran. Mohammad Reza Maraki is an Instructor of Material Engineering at Birjand University of Technology. He received his MSc in Material Engineering from Iran University of Science and Technology in 2002. His current research focuses on the welding process and fracture mechanic.

Research paper

COPYRIGHTS

© 2023 by the authors. Licensee Islamic Azad University Isfahan Branch. This article is an open access article distributed under the terms and conditions of the Creative Commons Attribution 4.0 International (CC BY 4.0)

<https://creativecommons.org/licenses/by/4.0/>



1 INTRODUCTION

The quality and mechanical properties of welds depend greatly on the presence of weld defects such as cavities, cracks, pores and components during traditional welding. Friction stir welding (FSW), invented in the 1990's by the Welding Institute (UK), is a solid-state welding process [1].

This welding method is used for welding materials with less weldability or almost welding by fusion and also for welding dissimilar alloys. Unlike traditional joint welding, in FSW, the bonding process takes place below the solid temperature, which causes less distortion, residual stress and various defects in the final products. FSW has other advantages such as simple sample preparation, precise external control and high connection speed, less energy consumption and less pollution reduction [2]. Given these advantages, FSW has received widespread attention as a process of joining similar and different alloys [3-6] for use in various industries, such as shipbuilding, vehicle construction, railways, aerospace and marine construction [7-9].

Recently, FSP has been widely used to fabricate Al-matrix surface nanocomposites with various nanoscale enhancers (including SiC [10-12], Al₂O₃ [13-15], B₄C [16-17], TiC [18], fullerene [19], SiO₂ [20-21], TiO₂ [22-24], TiB₂ [25], intermetallic [26]) or nanotubes (including single carbon nanotubes [27] and multi-wall carbon nanotube (CNT) [28-29]).

Nandipati et al. [30] investigated friction stir welded AA6061 metal matrix nanocomposites (MMNC) reinforced with SiC nanoparticles. Butola et al. [31] studied the measurement of residual stress on H13 tool steel during machining for fabrication of FSW/FSP tool pins. Zhang et al. [32] investigated microstructure, mechanical properties and fatigue crack growth behavior of friction stir welded joint of 6061-T6 aluminum alloy. Duan et al. [33] investigated microstructure, crystallography, and toughness in the nugget zone of friction stir welded high-strength pipeline steel. Shaikh et al. [34] used FSW for joining of high-density polyethylene (HDPE) composites that were formed through the additions of SiC, SiO₂, nano-alumina, and graphite powders during welding at the rotational speed of 1800 rpm, traveling speed of 16 mm/min and the other selected welding parameters. Khan et al. [35] investigated the effect of inter-cavity spacing in friction stir processed Al 5083 composites containing carbon nanotubes and boron carbide particles.

2 MATERIALS AND EXPERIMENTAL PROCEDURES

2.1. Nanoparticles

In this research, graphene and Al₂O₃ nanomaterials have been used. Graphene nanoplates with a purity of 99.9%, thickness of 2-4 μm, diameter less than 2 nm, specific surface area of 700 m²/g, black color and true density of 1.9-2.2 g/cm³ have been used. Aluminum oxide nanopowders (Al₂O₃, Gamma) with 99.9% purity, average particle size of 20-30 nm, specific surface area of 130-220 m²/g, white color, true density of 3.5-3.9 g/cm³, and crystal form nearly spherical (Gamma) have been used.

2.2. Friction Stir Processing/Welding (FSP/FSW)

In this paper, the alloy used for FSP/FSW is 7075-T651 aluminum. This alloy has heat treatment ability and the characteristic of T6 indicates heat treatment of solubilized and artificially aged type and the number 51 indicates de-stressing by stretching after heat treatment. Also, this alloy has excellent mechanical strength and is widely used in the aerospace industry. "Table 1" shows the chemical composition of this alloy, which was determined using chemical analysis with the Solaris OES Plus quantimeter manufactured by the Italian company GNR. The mechanical properties of the alloy are also given in "Table 2". The six plates used have dimensions of 120×120 mm and a thickness of 5 mm and the nanoparticles are inserted in cavities with a diameter of 2 mm and a depth of 3 mm (Figure 1). Cavities of diameter 2mm and depth 3mm were prepared on an Al7075 plate using a drilling machine. Two different spacing between the cavities were selected, i.e. 8mm and 10mm. Also a plate without inserting nanoparticles, FSP/FSW is performed.

Table 1 Chemical composition of 7075-T651 Aluminum Alloy

No.	E	%	No.	E	%
1	Fe	0.162	9	V	0.097
2	Cu	1.043	10	Zr	0.020
3	Mn	0.01	11	Ag	0.3
4	Mg	1.071	12	Ga	0.018
5	Cr	0.198	13	Sb	0.15
6	Zn	4.046	14	Bi	92.642
7	Ti	0.074	15	Al	
8	Pb	0.012	-	-	-

Table 2 Mechanical Properties of 7075-T651 Aluminum Alloy

Mechanical Properties	Value
Modulus of elasticity (GPa)	72
Yield strength (MPa)	529.78
Ultimate strength (MPa)	593.45
Poisson ratio	0.33
Micro Hardness (MicroVickers)	39
Elongation%	13.2

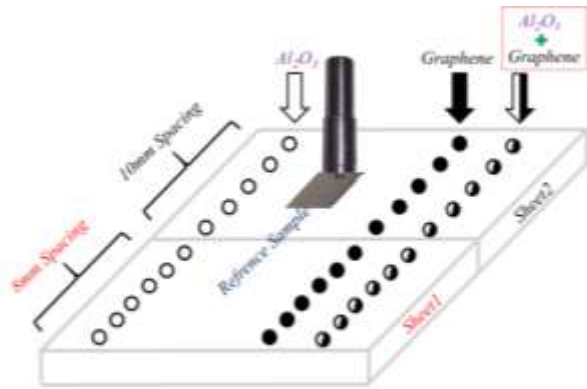


Fig. 1 Schematic of FSP.

For plate welding, a threaded pin shoulder was used to better dissolve the nanoparticles as shown in “Fig. 2”. The shoulder is made of SPK2436 steel alloy with a hardness of 50 Rockwell (HCR), the tool shoulder diameter is 20, pin diameter is 4 mm and pin height is 4 mm, and threads with a step of 1 mm are created on it while an angle of 2° was made from the shoulder to pin root to accumulate the possible spreading of reinforcement from cavities.



Fig. 2 Photographs of FSP/FSW shoulder.

The angle of deviation of the tool from the piece was also chosen to be 2 degrees. The proper angle between the tool pin and the workpiece as the tool shoulder travels through the FSW process allow the tool shoulder to cover the softened and moved material. At a deflection angle of 2 degrees, the materials that have become plastic when the tool penetrates and moves under the tool shoulder return to the workpiece with great pressure using the forging force behind the tool. To perform the process, FP4M manual milling machine was used. The FP4M milling machine has the ability to withstand the forces during the process and also the ability to move automatically in different directions. Since the workpiece fixture closes on the table, the machine table must be such that it does not vibrate during the process. If the machine is vibrating or has another defect, it has a great effect on the resulting process. Therefore, the obtained results will be with high error and unacceptable. The tool is advancing manually and slowly until it reaches the ideal linear speed. According to the material and thickness of the specimens, the rotational speed of 750 rpm, the advancing speed of the tool is 16 mm / min and the

penetration depth of 0.3 mm has been selected, (“Fig. 3”).



Fig. 3 Photograph of the process showing machine, tool and plate processed by FSP.

After the FSP/FSW, the specimens are first polished, next etched, and next prepared for macrography in the mount (“Fig. 4”). The different regions of the FSP/FSW are shown in “Fig. 5”.



Fig. 4 Specimens in mount for macrography



(a)



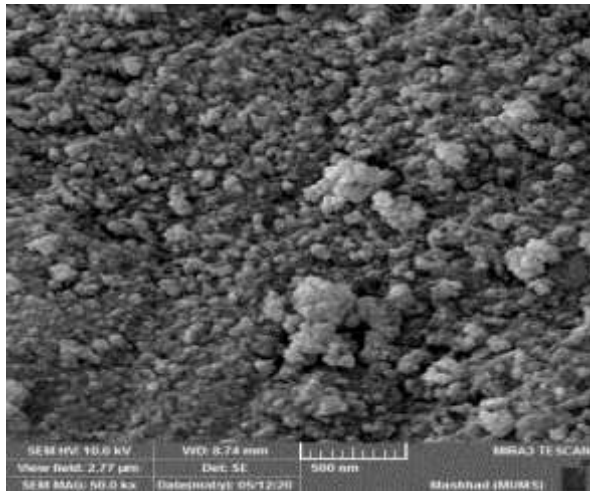
(b)



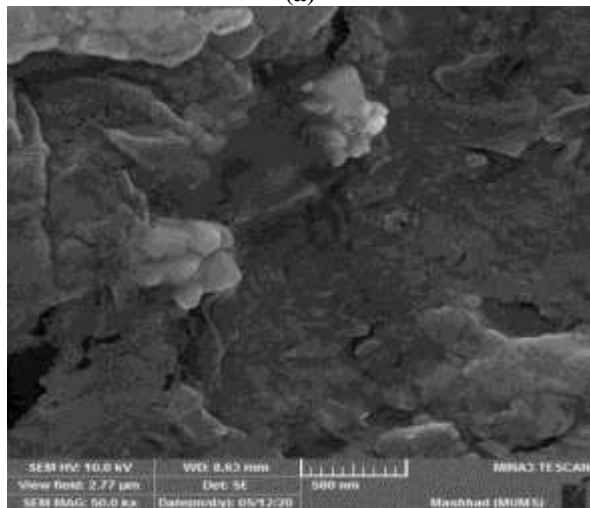
(c)

Fig. 5 Different FSP/FSW zones: (a): Base Metal, (b): HAZ and, (c): Weld Metal.

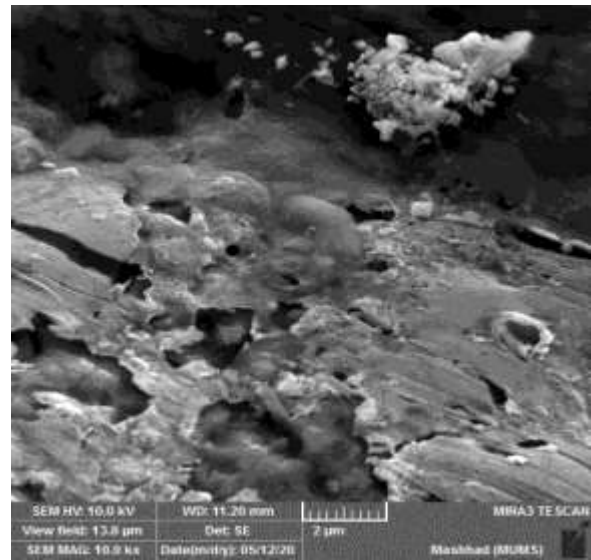
Imaging was also performed by scanning electron microscopy to observe the nanoparticles. Figure 6 shows the graphene and Al₂O₃ nanoparticles. The Al₂O₃ nanoparticles shown in “Fig. 6” correspond to a specimen with a distance of 8 mm showing that the nanoparticles have accumulated in one place due to their short distance from each other.



(a)



(b)



(c)

Fig. 6 SEM images of Al7075 reference with: (a): Al₂O₃ nanoparticles, (b): Graphene nanoplates, and (c): Al₂O₃ + Graphene.

2.3. Heat Treatment

After FSP/FSW process, from each group, three specimens were subjected to the T6 heat treatment cycle (dissolution at 480 ° C for 120 minutes and cooling in water and then precipitation at 120 ° C for 24 hours). Figure 7 shows a triple group of Charpy impact specimens before and after heat treatment.



(a)



(b)

Fig. 7 Charpy specimens: (a): before and, (b): after heat treatment.

The specimens are categorized according to “Table 3”.

Table 3 Grouping and naming specimens by adding nanoparticles

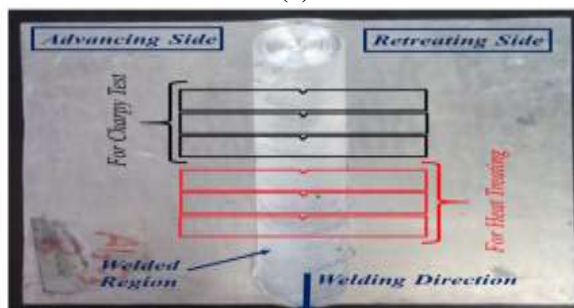
Number of Group	Nanoparticles	Distance cavities (mm)	Description
1	Gr + Al ₂ O ₃	8	-
2	Gr + Al ₂ O ₃	10	-
3	Al ₂ O ₃	8	-
4	Al ₂ O ₃	10	-
5	Graphene	8	-
6	Graphene	10	-
7	-	-	Specimen without nanoparticle (only FSP)
8	-	-	Specimen without nanoparticle and FSP

2.4. Charpy Impact Test

From 7075 aluminum plate, which made the friction stir welding process, as shown in “Fig. 8”, Charpy impact specimens are separated according to ASTM E23 so that the notch is in the center of the weld. Specimen notches can be pressed or machined (Chevron V-notch) according to the API 5L3 standard, which is created by a wirecut machine. The press notch created in the laboratory specimen by pressing the chisel is sharp enough and there are no residual stresses in the notch tip zone and also the type of notch can affect the fracture start energy [36].



(a)



(b)

Fig. 8 (a): The cavities to be prepared by drilling and Al7075 plate after drilling and, (b): after FSP and Schematic diagram of the Charpy specimens selector of the plate.

In this study, notches were created on the specimens using a wire-cut machine. Subsize specimens with dimensions of $55 \times 5 \times 10$ mm and notch angle of 45 degrees, notch tip radius of 0.25 mm, and notch depth of 2 mm have been made with sufficient precision and compliance with standard requirements. The specimens are then smoothed and polished by a grinding machine to smooth the surface.

Impact testing was performed using a 25-joules Charpy impact machine, C-shaped striker, hammer with an 8 mm radius at 23 ° C (“Fig. 9”).

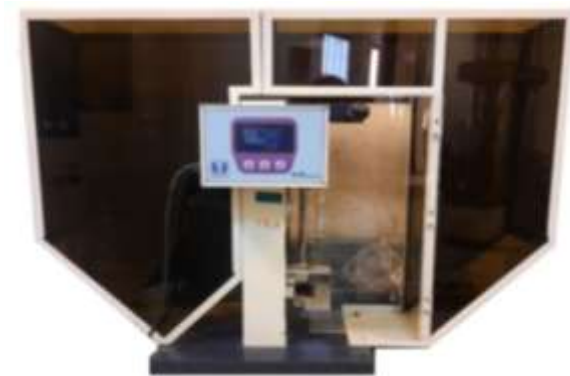


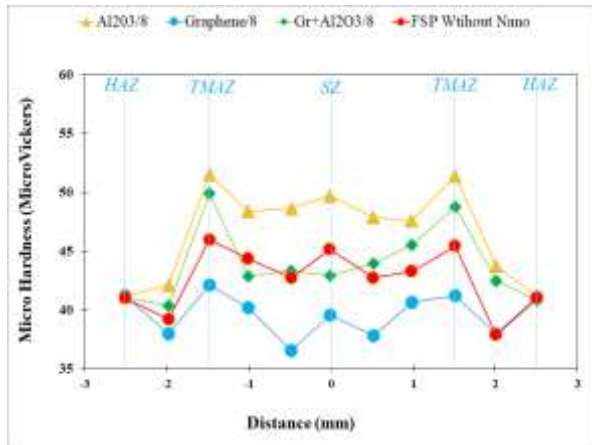
Fig. 9 Charpy impact machine used experimental test

Charpy impact test was repeated 3 times for each specimen and the average fracture energy obtained was reported as the final fracture energy.

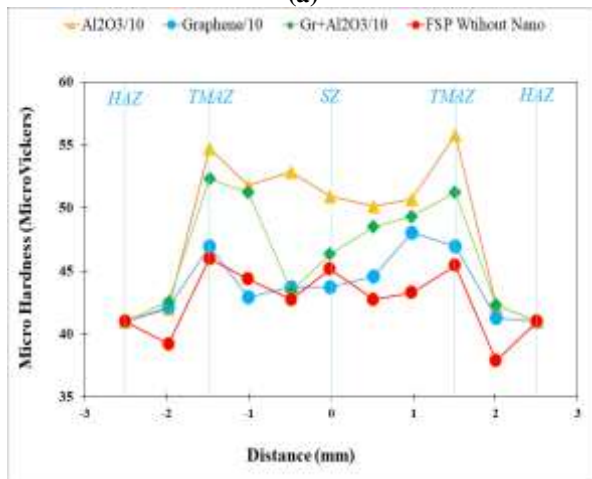
3 RESULTS AND DISCUSSION

3.1. Hardness

Six examples of FSP/FSW by Vickers microhardness have been investigated. Hardness results are reported in “Fig. 10”. Hardness is done in the zones of HAZ, TMAZ, SZ, TMAZ, HAZ and is W-shaped. In specimens with a distance between two cavities of 10 mm, the hardness in all three specimens of nanoparticles is higher than in specimens with a distance of 8 mm. Hardness results and microscopic observations show that nanoparticles have accumulated at shorter distances and reduced the hardness of the specimen. The best hardness results are for Al₂O₃ nanoparticles, then the combination of graphene nanoplate and Al₂O₃ nanoparticles. The lowest hardness is related to graphene nanoplates, which is even less hardness than the specimen without nanomaterials.



(a)



(b)

Fig. 10 Microhardness values of FSP/FSW composites: (a): 8mm spacing and, (b): 10mm spacing specimens.

3.2. Charpy Impact Test

Seven specimens of friction stir welding were tested by a 25-joule Charpy impact machine. The results of the Charpy impact test are reported in “Fig. 11”.

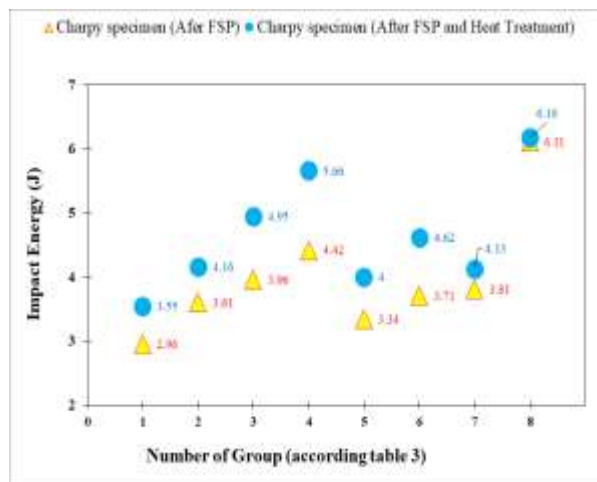


Fig. 11 Result of Charpy impact test.

Experimental results show that the fracture energy of specimens with nanomaterials at a distance of 10 mm is higher. This shows that in specimens with a distance of 8 mm nanomaterials accumulated and reduced the fracture energy.

In all specimens, after heat treatment, higher fracture energy was reported, which indicates that heat treatment has caused the nanomaterials to penetrate well into the material and become part of the material structure.

The highest fracture energy is related to the specimen in which the Al₂O₃ nanoparticles are set at a distance of 10 mm. The lowest fracture energy is related to a specimen that combines Al₂O₃ and graphene nanomaterials at a distance of 8 mm, which is even lower in a specimen where the FSP/FSW is performed alone. In all cases, the fracture energy of specimens with a distance of 10 mm is higher than that of specimens with a distance of 8 mm. This is due to the accumulation of nanomaterials at shorter distances, which reduces the strength of the material.

4 CONCLUSIONS

In the present study, the Effect of inter-cavity spacing and heat treatment in friction stir Processing/welding (FSP/FSW) Al₇₀₇₅ composites containing Al₂O₃ and Graphene nanomaterials using Charpy impact test was investigated. 24 specimens were tested in eight specimens series (each specimen 3 times) with standard subsize specimens. The specimens were also heat treated and Charpy tested again. The Charpy impact machine used in this experiment had the capacity of 25 joules, which is selected according to ASTM E23. Also, fractography of the samples was performed by optical microscopy and SEM. the results are summarized as follows:

- 1- The hardness in specimens with a distance of 10 mm is higher than the specimens with a distance of 8 mm in all three specimens with different nanoparticles.
- 2- Hardness results and microscopic observations show that nanoparticles have accumulated at shorter distances and reduced the hardness of the specimen.
- 3- The best hardness results are for alumina nanoparticles, then the combination of graphene nanoplate and Al₂O₃ nanoparticles. The lowest hardness is related to graphene nanoplates, which is even less hardness than the specimen without nanomaterials.
- 4- In the Charpy test, all specimens reported higher fracture energy after heat treatment, indicating that heat treatment caused the nanomaterials to penetrate well into the material and become part of the material structure.

5- The highest fracture energy is related to the specimen where the Al₂O₃ nanoparticles are placed at a distance of 10 mm.

6- The lowest fracture energy is related to a specimen that combines Al₂O₃ and graphene nanomaterials at a distance of 8 mm, which is even lower in a specimen where the FSP/FSW is performed alone.

7- In all cases, the fracture energy of specimens with a distance of 10 mm is higher than that of specimens with a distance of 8 mm. This is due to the accumulation of nanomaterials at shorter distances, which reduces the strength of the material.

REFERENCES

- [1] Wahid, M. A., Khan, Z. A., and Siddiquee, A. N., Review on Underwater Friction Stir Welding: A Variant of Friction Stir Welding with Great Potential of Improving Joint Properties Transactions of Nonferrous Metals Society of China, Vol. 28, No. 2, 2018, pp. 193-219.
- [2] Subramanya, P., Amar, M., Arun, S., Mervin, H., and Shrikantha, R., Friction Stir Welding of Aluminium Matrix Composites—A Review, MATEC Web Conf., Vol. 144, 2018, pp. 03002, <http://dx.doi.org/10.1051/mateconf/201814403002>
- [3] Murr, L., A Review of FSW Research on Dissimilar Metal and Alloy Systems, J. Mater. Eng. Perform., Vol. 19, No. 8, 2010, pp. 1071-1089, <http://dx.doi.org/10.1007/s11665-010-9598-0>.
- [4] Chen, T., Process Parameters Study on FSW Joint of Dissimilar Metals for Aluminum–Steel, J. Mater. Sci., Vol. 44, No. 10, 2009, pp. 2573-2580, <http://dx.doi.org/10.1007/s10853-009-3336-8>.
- [5] Carlone, P., Astarita, A., Palazzo, G. S., Paradiso, V., and Squillace, A., Microstructural Aspects in Al–Cu Dissimilar Joining by FSW, Int. J. Adv. Manuf. Technol., Vol. 79, No. 5-8, 2015, pp. 1109-1116, <http://dx.doi.org/10.1007/s00170-015-6874-z>.
- [6] Moghadam, D. G., Farhangdoost, K., Influence of Welding Parameters on Fracture Toughness and Fatigue Crack Growth Rate in Friction Stir Welded Nugget of 2024-T351 Aluminum Alloy Joints, Trans. Nonferrous Met. Soc. China, Vol. 26, No. 10, 2016, pp. 2567-2585, [http://dx.doi.org/10.1016/S1003-6326\(16\)64383-2](http://dx.doi.org/10.1016/S1003-6326(16)64383-2).
- [7] Zhao, J., Jiang, F., Jian, H., Wen, K., Jiang, L., and Chen, X., Comparative Investigation of Tungsten Inert Gas and Friction Stir Welding Characteristics of Al–Mg–Sc Alloy Plates, Mater. Des. Vol. 31, No. 1, 2010, pp. 306-311, <http://dx.doi.org/10.1016/j.matdes.2009.06.012>.
- [8] Cavaliere, P., Cabibbo, M., Panella, F., and Squillace, A., 2198 Al–Li Plates Joined by Friction Stir Welding: Mechanical and Microstructural Behavior, Mater. Des., Vol. 30, No. 9, 2009, pp. 3622-3631, <http://dx.doi.org/10.1016/j.matdes.2009.02.021>.
- [9] Thomas, W., Nicholas, E., Friction Stir Welding for The Transportation Industries, Mater. Des., Vol. 18, No. 4-6, 1997, pp. 269-273.
- [10] Ni, D., Chen, D., Wang, D., Xiao, B., and Ma, Z., Influence of Microstructural Evolution on Tensile Properties of Friction Stir Welded Joint of Rolled SiCp/AA2009-T351 Sheet, Mater. Des., Vol. 51, 2013, pp. 199-205, <http://dx.doi.org/10.1016/j.matdes.2013.04.027>.
- [11] Khodabakhshi, F., Gerlich, A., and Švec, P., Fabrication of a High Strength Ultra-Fine-Grained Al–Mg–SiC Nanocomposite by Multi-Step Friction-Stir Processing, Mater. Sci. Eng. A, Vol. 698, 2017, pp. 313-325, <http://dx.doi.org/10.1016/j.msea.2017.05.065>.
- [12] Khodabakhshi, F., Simchi, A., Kokabi, A., and Gerlich, A., Similar and Dissimilar Friction-Stir Welding of an PM Aluminum-Matrix Hybrid Nanocomposite and Commercial Pure Aluminum: Microstructure and Mechanical Properties, Mater. Sci. Eng. A, Vol. 666, 2016, pp. 225-237, <http://dx.doi.org/10.1016/j.msea.2016.04.078>.
- [13] Ashjari, M., Asl, A. M., and Rouhi, S., Experimental Investigation on The Effect of Process Environment on The Mechanical Properties of AA5083/Al₂O₃ Nanocomposite Fabricated Via Friction Stir Processing, Mater. Sci. Eng. A, Vol. 645, 2015, pp. 40-46, <http://dx.doi.org/10.1016/j.msea.2015.07.093>.
- [14] Khodabakhshi, F., Yazdabadi, H. G., Kokabi, A., and Simchi, A., Friction Stir Welding of a P/M Al–Al₂O₃ Nanocomposite: Microstructure and Mechanical Properties, Mater. Sci. Eng. A, Vol. 585, 2013, pp. 222-232, <http://dx.doi.org/10.1016/j.msea.2013.07.062>.
- [15] Khodabakhshi, F., Simchi, A., Kokabi, A., Gerlich, A., Nosko, M., and Švec, P., Influence of Hard Inclusions on Microstructural Characteristics and Textural Components During Dissimilar Friction-Stir Welding of an PM Al–Al₂O₃–SiC Hybrid Nanocomposite with AA1050 Alloy, Sci. Technol. Weld. Join., Vol. 22, No. 5, 2017, pp. 412-427, <http://dx.doi.org/10.1080/13621718.2016.1251714>.
- [16] Narimani, M., Lotfi, B., and Sadeghian, Z., Evaluation of the Microstructure and Wear Behavior of AA6063-B4C/TiB₂ Mono and Hybrid Composite Layers Produced by Friction Stir Processing, Surf. Coat. Tech., Vol. 285, 2016, pp. 1-10, <http://dx.doi.org/10.1016/j.surfcoat.2015.11.015>.
- [17] Yuvaraj, N., Aravindan, S., Fabrication of Al5083/B4C Surface Composite by Friction Stir Processing and Its Tribological Characterization Journal of Materials Research and Technology, Vol. 4, No. 4, 2015, pp. 398-410, <http://dx.doi.org/10.1016/j.jmrt.2015.02.006>.
- [18] Rejil, C. M., Dinaharan, I., Vijay, S., and Murugan, N., Microstructure and Sliding Wear Behavior of AA6360/(TiC+ B4C) Hybrid Surface Composite Layer Synthesized by Friction Stir Processing on Aluminum Substrate, Mater. Sci. Eng. A, Vol. 552, 2012, pp. 336-344, <http://dx.doi.org/10.1016/j.msea.2012.05.049>.
- [19] Morisada, Y., Fujii, H., Nagaoka, T., Nogiand K., Fukusumi, M., Fullerene/A5083 Composites Fabricated by Material Flow During Friction Stir Processing, Compos., Part A Appl. Sci. Manuf., Vol. 38, No. 10, 2007, pp. 2097-2101,

- <http://dx.doi.org/10.1016/j.compositesa.2007.07.004>.
- [20] Ramesh, S., Sivasamy, A., Rhee, K., Park, S., and Hui, D., Preparation and Characterization of Maleimide–Polystyrene/SiO₂–Al₂O₃ Hybrid Nanocomposites by An In-Situ Sol-Gel Process and Its Antimicrobial Activity, *Compos., Part B Eng.*, Vol. 75, 2015, pp. 167-175, <http://dx.doi.org/10.1016/j.compositesb.2015.01.040>.
- [21] You, G., Ho, N., and Kao, P., In-Situ Formation of Al₂O₃ Nanoparticles During Friction Stir Processing of AlSiO₂ Composite, *Mater. Charact.*, Vol. 80, 2013, pp. 1-8, <http://dx.doi.org/10.1016/j.matchar.2013.03.004>.
- [22] Khodabakhshi, F., Gerlich, A., Simchi, A., and Kokabi, A., Hot Deformation Behavior of An Aluminum-Matrix Hybrid Nanocomposite Fabricated by Friction Stir Processing, *Mater. Sci. Eng. A*, Vol. 626, 2015, pp. 458-466, <http://dx.doi.org/10.1016/j.msea.2014.12.110>.
- [23] Khodabakhshi, F., Gerlich, A., Simchi, A., and Kokabi, A., Cryogenic Friction-Stir Processing of Ultrafine-Grained Al–Mg–TiO₂ Nanocomposites, *Mater. Sci. Eng. A*, Vol. 620, 2015, pp. 471-482, <http://dx.doi.org/10.1016/j.msea.2014.10.048>.
- [24] Khodabakhshi, F., Simchi, A., Kokabi, A., Sadeghahmadi, M., and Gerlich, A., Reactive Friction Stir Processing of AA 5052–TiO₂ Nanocomposite: Process–Microstructure–Mechanical Characteristics, *Mater. Sci. Technol.*, Vol. 31, No. 4, 2015, pp. 426-435, <http://dx.doi.org/10.1179/1743284714Y.0000000573>.
- [25] Eskandari, H., Taheri, R., and Khodabakhshi, F., Friction-Stir Processing of an AA8026-TiB₂-Al₂O₃ Hybrid Nanocomposite: Microstructural Developments and Mechanical Properties, *Mater. Sci. Eng. A*, Vol. 660, 2016, pp. 84-96, <http://dx.doi.org/10.1016/j.msea.2016.02.081>.
- [26] Khodabakhshi, F., Simchi, A., Kokabi, A., and Gerlich, A., Friction Stir Processing of An Aluminum-Magnesium Alloy with Pre-Placing Elemental Titanium Powder: In-Situ Formation of an Al₃Ti Reinforced Nanocomposite and Materials Characterization, *Mater. Charact.*, Vol. 108, 2015, pp. 102-114, <http://dx.doi.org/10.1016/j.matchar.2015.08.016>.
- [27] Liu, Z., Xiao, B., Wang, W., and Ma, Z., Singly Dispersed Carbon Nanotube/Aluminum Composites Fabricated by Powder Metallurgy Combined with Friction Stir Processing, *Carbon*, Vol. 50, No. 5, 2012, pp. 1843-1852, <http://dx.doi.org/10.1016/j.carbon.2011.12.034>.
- [28] Kim, W., Lee, T., and Han, S., Multi-Layer Graphene/Copper Composites: Preparation Using High-Ratio Differential Speed Rolling, Microstructure and Mechanical Properties, *Carbon*, vol. 69, 2014, pp. 55-65, <http://dx.doi.org/10.1016/j.carbon.2013.11.058>.
- [29] Kondoh, K., Fukuda, H., Umeda, J., Imai, H., and Fugetsu, B., Microstructural and Mechanical Behavior of Multi-Walled Carbon Nanotubes Reinforced Al–Mg–Si Alloy Composites in Aging Treatment, *Carbon*, Vol. 72, 2014, pp. 15-21, <http://dx.doi.org/10.1016/j.carbon.2014.01.013>.
- [30] Nandipati, G., Damera, N., and Nallu, R., Effect of Microstructural Changes on Mechanical Properties of Friction Stir Welded Nano SiC Reinforced AA6061 Composite, *Int. J. Eng. Sci. Technol.*, Vol. 2, No. 11, 2010, pp. 6491-6499.
- [31] Butola, R., Choudhary, N., Kumar, R., Kumar Mouria, P., Zubair, M., Ranganath, M., and Singari, M., Measurement of Residual Stress on H13 Tool Steel During Machining for Fabrication of FSW/FSP Tool Pins, *Materials Today: Proceedings*, Vol. 43, No. 1, 2021, pp. 256-262.
- [32] Zhang, L., Zhong, H., Li, Sh., Zhao, H., Chen, J., and Qi, L., Microstructure, Mechanical Properties and Fatigue Crack Growth Behavior of Friction Stir Welded Joint of 6061-T6 Aluminum Alloy, *International Journal of Fatigue*, Vol. 135, 2020, 105556, ISSN 0142.
- [33] Duan, R. H., Xie, G. M., Luo, Z. A., Xue, P., Wang, C., Misra, R. D. K., and Wang, G. D., Microstructure, Crystallography, And Toughness in Nugget Zone of Friction Stir Welded High-Strength Pipeline Steel, *Materials Science and Engineering: A*, Vol. 791, 2020, 139620, ISSN 0921-5093.
- [34] Shaikh, A. S., Tahir, M. S., and Qureshi, M. K. A., Experimental Investigation of Mechanical Properties of Friction Stir Welded HDPE with Additions of Silicon Carbide, Silica, Nano-Alumina, And Graphite, *Materials Science and Technology, Joining of Advanced and Specialty Materials*, 2012, pp. 316-323.
- [35] Khan, M., Rehman, A., Aziz, T., Shahzad, M., Naveed, K., and Subhani, T., Effect of Inter-Cavity Spacing in Friction Stir Processed Al 5083 Composites Containing Carbon Nanotubes and Boron Carbide Particles, *Journal of Materials Processing Technology*, Vol. 253, 2018, pp. 72-85, ISSN 0924-0136.
- [36] Majidi, A., Hashemi, S. H., Study of Macroscopic Fracture Surface Characteristics of Spiral Welded API X65 Gas Transportation Pipeline Steel, *Modares Mechanical Engineering*, Vol. 17, No. 11, 2018, pp. 219-228.